Mecánica Computacional Vol. XXIV
A. Larreteguy (Editor)
Buenos Aires, Argentina, Noviembre 2005

A THREE-DIMENSIONAL MOVING FINITE ELEMENT METHOD BASED ON A POSTERIORI ERROR ESTIMATION

Gustavo Bono[*] and Armando M. Awruch[†]

[*] Graduate Program in Mechanical Engineering
Federal University of Rio Grande do Sul,
Av. Sarmento Leite 425 (CEP: 90050-170), Porto Alegre, RS, Brazil
e-mail: gbono@mecanica.ufrgs.br

[†] Applied and Computational Mechanical Center
Federal University of Rio Grande do Sul,
Av. Osvaldo Aranha 99, 3º andar (CEP: 90035-190), Porto Alegre, RS, Brazil
e-mail: amawruch@ufrgs.br

Key words: Adaptive mesh strategy, High compressible flows, Finite element method.

Abstract. *A moving finite element method based on a posteriori error estimate is presented for three-dimensional compressible flows, with emphasis on shock waves. The adaptation procedure uses an interpolation error estimate whose magnitude and direction are controlled by the Hessian, containing second derivatives of the specific mass. This error is projected over mesh edges and drive the nodal movement scheme to satisfy an optimal mesh criterion. While traditionally the optimal mesh criterion is one in which the error is equidistributed over the elements, in this work the error is equidistributed over the edges. Mesh anisotropy is avoided employing a formulation based in variational principles. Finally, numerical result obtained with current method are presented and analyzed for several examples.*

1 INTRODUCTION

The numerical solution of complex problems in many engineering fields normally requires the uses of a large number of mesh points to accurately capture phenomena exhibiting high gradients of one or more variables such as those appearing in boundary layers, regions with stress concentration, shock waves, etc.. As regions where the phenomena take place are not known *a priori* in many case, it is rarely feasible to create a suitable initial mesh with small elements at the corresponding location where high gradients may be found. Several approaches have been employed for both structured and unstructured mesh adaptation. The most widely used approaches consist in nodal re-allocation, automatic mesh refinement/unrefinement and changes of the approximation order of the variables. Sometimes it could be appropriated to use simultaneously more than one of these approaches. Most of these subjects are well summarized in Löhner[1], where many references are given.

A strategy for mesh adaptation, using only mesh movement and nodal re-allocation, has the advantage that the mesh connectivity and number of elements and nodes do not vary with respect to the initial mesh and hence computational cost does not increase when a new flowfield is calculated on the adapted mesh. The node movement technique was originally presented by Gnoffo[2], and was after generalized by Nakahashi and Deiwert[3], for fluid flow problems. The scheme used by these authors are based in the spring analogy, where the mesh is viewed as a set of springs with their constants representing error measures. Each apex (or node) is moved until equilibrium are reached by the spring forces. The refinement technique using exclusively nodal movement has been less popular in the finite element community; the main difficulty seems to be the lack of a reliable and general procedure to determine the mesh movement. Nevertheless, as this method is easy to implemented and inexpensive, because only the initial mesh with non complex data structure is needed to originate continuos changes or the mesh in the time-space domain, it is worthwhile to employ this technique whenever it is possible. Hawken et al.[4] presented a review of adaptive node-movement techniques in finite elements and finite differences. Ait-Ali-Yahia et al.[5] studied a methodology for quadrilateral elements using an edge-based error estimate, but high aspect ratios (such as 50 for some elements) were obtained. Tam et al. [6] extended this methodology for 3-D hexahedral elements, where mesh refinement is also considered.

In the presented work a node-movement technique is implemented for compressible flows characterized by strong shock waves, analized with the Finite Element Method (FEM) using hexahedral isoparametric elements with eight nodes. An edge-based error estimate drives nodal movement to satisfy an optimal mesh criterion. The error is equidistributed over the edges and an initial mesh is continuously adapted during the solution process, keeping as well as possible mesh smoothness and local orthogonality with an unconstrained optimization method. An Arbitrary Langrangean-Eulerian (ALE) description is used in order to obtain a conservative computation of the flow when the adaptive mesh procedure transport informations from the old to the new mesh. Classical computational fluid dynamics problems such as the supersonic flow over a ramp, and the supersonic flows around a cylinder are presented to apply the proposed methodology.

2 THE NUMERICAL SCHEME

The mass, momentum and energy conservation equations for compressible flows, neglecting viscous and heat diffusion term using an ALE description, may be written in a compact form as:

$$\frac{\partial \mathbf{U}}{\partial t}+\frac{\partial \mathbf{F}_i}{\partial x_i}-w_i\frac{\partial \mathbf{U}}{\partial x_i}=0 \qquad (i=1,2,3) \tag{1}$$

with,

$$\mathbf{U}=\begin{Bmatrix}\rho\\ \rho v_1\\ \rho v_2\\ \rho v_3\\ \rho e\end{Bmatrix}; \qquad \mathbf{F}_i=\begin{Bmatrix}\rho v_i\\ \rho v_1 v_i+p\delta_{i1}\\ \rho v_2 v_i+p\delta_{i2}\\ \rho v_3 v_i+p\delta_{i3}\\ v_i\left(\rho e+p\right)\end{Bmatrix} \tag{2}$$

where $\mathbf{U}$ and $\mathbf{F}_i$ are vectors containing field and flux variables, respectively. In these expressions, v_i and w_i are the fluid and mesh velocity components in the direction of the spatial coordinates x_i, respectively, ρ is the specific mass, p is the thermodynamic pressure and e is the total energy. Finally, δ_{ij} is the Kronecker delta and t is the time coordinate.

Equation (1) is complemented by the equation of state for an ideal gas. The problem is completely defined when initial and boundary conditions are added to these equations.

The system of partial differential equations is solved with an explicit scheme using the finite element method, employing a Taylor series and the classical Bubnov-Galerkin method[1,7] for time and space discretization, respectively. An isoparametric eight node hexahedrical element is used and the corresponding element matrices are obtained analytically employing reduced numerical integration. This code has been validated against analytical and experimental results for several compressible flows (Kessler and Awruch[8], Bono[9]).

3 MESH ADAPTION

3.1 The error estimation

Assume a one-dimensional problem, in which a variable ρ is approximated by ρ_h using piecewise linear interpolation functions. The root mean square error interpolation in an element e is given by (Peraire et al.[10]):

$$E_e^{rms}=\frac{1}{\sqrt{120}}h^2\left|\frac{d^2\rho_h}{dx^2}\right| \tag{3}$$

provided that the approximation is exact at the nodes. In Eq. (3), h is the element length. An optimal mesh is obtained when the error is equidistributed, that is:

$$h^2 \left| \frac{d^2 \rho_h}{dx^2} \right| = C \tag{4}$$

where C is a specific tolerance. For a three-dimensional problem, the second derivative of the variable approximated by ρ_h with respect to a direction defined by the versor $\boldsymbol{V}$ is given by:

$$\frac{\partial^2 \rho_h}{\partial \boldsymbol{V}^2} = \boldsymbol{V}^T \boldsymbol{H}\, \boldsymbol{V} \tag{5}$$

where $\boldsymbol{H}$ is the Hessian matrix. As ρ_h is interpolated with linear shape functions, the second derivative of ρ_h at a node I can be calculated using a weak formulation[6] obtaining:

$$\left. \frac{\partial^2 \rho_h}{\partial {x_j}^2} \right|_I = \boldsymbol{M}^{-1} \left\{ \left[-\int_{\Omega_I} \left(\frac{\partial \phi^T}{\partial x_j} \phi \right) d\Omega \right] \left(\frac{\partial \rho_h}{\partial x_i} \right) + \left[\int_{\Gamma_I} \phi^T \phi\, n_j \; d\Gamma \right] \left(\frac{\partial \rho_h}{\partial x_i} \right) \right\} \tag{6}$$

where $\boldsymbol{M}^{-1}$ is the inverse of the mass matrix, which is given by:

$$\boldsymbol{M}^{-1} = \left(\int_{\Omega_I} \phi^T \phi \;\, d\Omega \right)^{-1} \tag{7}$$

where ϕ is a vector containing the shape functions, Ω_I is the volume of all the elements sharing the node I and Γ_I is the corresponding boundary. I varies from 1 until the total number of nodes in the finite element mesh, n_j represents the cossine of the angle formed by a normal axis to Γ_I with the coordinates axis x_j. The first derivatives of ρ_h are nodal values that can be obtained using a smoothing process based in the mean square method. In Eq. (6) as well as in the smoothing process to obtain values of $\partial \rho_h / \partial x_j$ at the nodes, the lumped mass matrix may be used instead the consistent mass matrix, indicated in Eq. (7).

The matrix $\boldsymbol{H}$ can be diagonalized and, in this case, Eq. (5) may be written as follows:

$$\frac{\partial^2 \rho_h}{\partial \boldsymbol{V}^2} = \boldsymbol{V}^T \boldsymbol{R}\, \boldsymbol{\Lambda} \boldsymbol{R}^T\, \boldsymbol{V} \tag{8}$$

Where $\boldsymbol{\Lambda}$ is a diagonal matrix containing the eigenvalues of $\boldsymbol{H}$ and $\boldsymbol{R}$ contains the corresponding eigenvectors. As the error must be positive, the original matrix $\boldsymbol{H}$ is substituted by $\bar{\boldsymbol{H}}$, where the absolute values of the eigenvalues are taken. It results in:

$$\left| \frac{\partial^2 \rho_h}{\partial \boldsymbol{V}^2} \right| = \left| \boldsymbol{V}^T \boldsymbol{H}\, \boldsymbol{V} \right| \le \boldsymbol{V}^T \bar{\boldsymbol{H}}\, \boldsymbol{V} = \boldsymbol{V}^T \left(\boldsymbol{R} \left| \boldsymbol{\Lambda} \right| \boldsymbol{R}^T \right) \boldsymbol{V} \tag{9}$$

In the current approach, the error, given by Eq. (4), is equidistributed over the mesh edges, where h is the Euclidian length of an element edge, and the second derivative of ρ_h is now given by Eq. (9), where $\boldsymbol{V}$ is a unit vectors that support this specific edge. An optimal mesh would by defined as the one in which all the edges have the same length in the Riemann metric defined by $\boldsymbol{V}^T \bar{\boldsymbol{H}} \boldsymbol{V}$. Thus the edge-baser error estimate is computed evaluating numerically the following expression on each edge *i-j*:

$$d^{\,i-j} = \int_0^h \left[\left(\boldsymbol{x}_j - \boldsymbol{x}_i \right)^T \bar{\boldsymbol{H}}(s) \left(\boldsymbol{x}_j - \boldsymbol{x}_i \right) \right]^{1/2} ds \tag{10}$$

where $\left\| x_j - x_i \right\| = h$ and s is an independent variable, such as $0 \le s \le h$.

3.2 The mesh movement

In general, the adaptive process with nodal redistribution consists of the three main steps. The first step is to define an appropriated monitoring function, which is representative of important solution features. The second, and probably the most crucial step, is to redistribute the node in the computational domain in a manner consistent with the aforestated monitoring function. It is crucial that the geometric fidelity of solid boundaries be maintained during the redistribution process. Mesh quality, measured by orthogonality and smoothness, must be also maintained. In third step the metric terms are modified to reflect mesh movement with a consistent node speed to re-evaluate the flow variables at the new mesh using an appropriate scheme.

Brackbill and Saltzman[11] formulated the grid equations in a variational form to produce satisfactory mesh concentration while maintaining relatively good smoothness and orthogonality. Their approaches has become one of the most popular methods used for mesh generation and adaptation in the past. In order to improve computational efficiency and reliability of this method Carcaillet et al.[12] and Kennon and Dulikravich[13] adopted a more heuristic formulation for the local adaptation problem.

Consider a typical cell, formed by eight element in the three-dimensional case, as it is shown in Figure 1. $P_{ijk} = P\,(\boldsymbol{x}_{ijk})$ is a common node belonging to the eight elements forming the cell, which is connected to the other nodes by straight segments defined as position vectors. The six position vectors with origin at the node P_{ijk} are used to form twelve scalar products, which are squared and summed to control orthogonality, OR_{ijk}, of the typical cell. A measure quantifying the local smoothness, SM_{ijk}, is given by the sum of the six scalar products of the position vectors forming the typical cell. The sum will be zero if all adjacent elements are equal volume. Details of local orthogonality and local smoothness formulation can be found in Kennon and Dulikravich [13].

The global objective function to be minimized is given by:

$$\min_{\boldsymbol{x}_I} \boldsymbol{F} = \min_{\boldsymbol{x}_I} \sum_{i=1}^{l} \sum_{j=1}^{m} \sum_{k=1}^{n} \left[\delta \cdot \frac{OR_{ijk}}{OR_{\max}} + (1-\delta) \frac{SM_{ijk}}{SM_{\max}} + \beta \cdot d_{ijk} \right] \tag{11}$$

with $0 \le \delta \le 1$ and $0 \le \beta \le 1$, where δ and β are weighting parameters, while OR_{max} and SM_{max} are the largest values or OR_{ijk} and SM_{ijk}, respectively, in order to ensure values of the same order in Eq. (11); l, m and n are the number of nodes in directions i, j and k, respectively. In Eq. (11), d_{ijk} is obtained by the summ of the square values of the edge-based error-estimate, given in Eq. (10), for all the element edges having P_{ijk} as a common end.

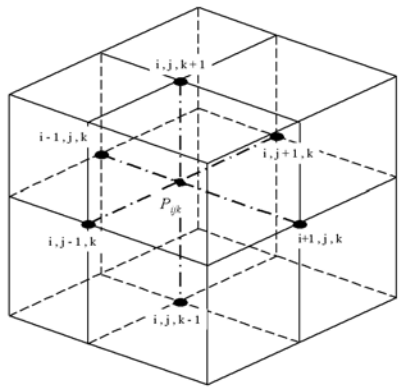

Figure 1: Typical cell defined for three-dimensional case

The conjugated gradient method, proposed by Fletcher-Reeves [14], is used to vary the node positions until the non-linear objective function $\boldsymbol{F}\left\{\left(\boldsymbol{x}_{ijk}\right): 1 \le i \le l, \quad 1 \le j \le m, \quad 1 \le k \le n\right\}$ is minimized. The conjugated gradient method has the following forms:

$$\boldsymbol{x}_{p+1} = \boldsymbol{x}_p + \alpha_p \boldsymbol{d}_p \tag{12}$$

with,

$$\boldsymbol{d}_p = \begin{cases} \boldsymbol{-g}_p & \text{for} \quad p = 1, \\ \boldsymbol{-g}_p + \beta_p \boldsymbol{d}_{p-1} & \text{for} \quad p \ge 2, \end{cases} \tag{13}$$

where $\boldsymbol{g}_p = \nabla F\left(\boldsymbol{x}_p\right)$, α_p is a scalar and β_p is a step size obtained by means of a one-dimensional search for descent direction and called exact line search.

Vector $\boldsymbol{d}_p$ is a descent direction if $\left\langle \boldsymbol{g}_p, \boldsymbol{d}_p \right\rangle < 0$, where $\left\langle \bullet, \bullet \right\rangle$ is the scalar product. This relationship may be written as:

$$\boldsymbol{F}_p^{'}\left(0\right) < 0 \tag{14}$$

with $\boldsymbol{F}_p^{'}\left(\alpha_p\right) = \left\langle \boldsymbol{g}_p\left(\alpha_p\right), \boldsymbol{d}_p \right\rangle$, since we consider functions of the scalar α_p verifying:

$$\boldsymbol{F}_p\left(\alpha_p\right) = \boldsymbol{F}_p\left(\boldsymbol{x}_p + \alpha_p \boldsymbol{d}_p\right) \quad \text{and} \quad \boldsymbol{g}_p\left(\alpha_p\right) = \boldsymbol{g}_p\left(\boldsymbol{x}_p + \alpha_p \boldsymbol{d}_p\right) \tag{15}$$

We note that $\boldsymbol{F}_p(0)=\boldsymbol{F}_p$ and $\boldsymbol{g}_p(0)=\boldsymbol{g}_p$. Moreover, the requirement $\boldsymbol{F}_{p+1}<\boldsymbol{F}_p$ translating decrease of $\boldsymbol{F}$ at each iteration is unsatisfactory since the decrease can be negligible when compared with reduction which can be obtained in an optimum reduction process based on exact line search. This exact line search supposes that α_p satisfies the Strong Wolfe conditions:

$$\begin{aligned} &\boldsymbol{F}_p(\alpha_p)\le \boldsymbol{F}_p(0)+\mu\,\alpha_p\,\boldsymbol{F}_p^{'}(0) \\ &\left|\boldsymbol{F}_p^{'}(\alpha_p)\right|\le \eta\left|\boldsymbol{F}_p^{'}(0)\right| \end{aligned} \qquad \text{with} \quad 0<\mu<\eta<1/2 \tag{16}$$

Value for β_p was proposed by Fletcher-Reeves:

$$\beta_p^{FR}=\frac{\left\langle \boldsymbol{g}_p,\boldsymbol{g}_p\right\rangle}{\left\langle \boldsymbol{g}_{p-1},\boldsymbol{g}_{p-1}\right\rangle}\ge 0 \tag{17}$$

Restrictions are prescribed to the motion of the nodes belonging to the boundaries surfaces.

4 NUMERICAL EXAMPLES

For all test cases investigated, the specific mass is the variable used for the error estimate, and the adaptive process was applied when a relatively small value of the residual value corresponding to ρ was reached.

The following values were adapted for the weighting parameters in Eq. (11): δ = 0.5 and β = 1.0. The fluid properties are assumed to be constant with γ = 1.4. Boundary nodes are free to move on the corresponding boundary planes or surfaces.

4.1 Steady supersonic flow over a ramp

In this example, the current methodology is applied to a steady supersonic flow over a ramp forming 16º with the horizontal axis. This example tests certain features of the algorithm, including the resolution of the oblique shock and its proper angle.

The freestream has a Mach number equal to 3.0 and dimensionless specific mass equal to 1.0. This case was computed using an mesh with 42 x 26 x 4 elements.

In Fig. 2 the initial and final meshes are shown, and it is observed that the elements are aligned with the shock wave conserving a mesh with a good quality.

The final mesh with some details is presented in Fig. 3 and the specific mass distribution for y = 0.5 is shown in Fig. 4, it is observed that the adaptive method improves results in regions with strong gradients. This result agrees well with the analytical values presented in the NACA Report 1135 [15].

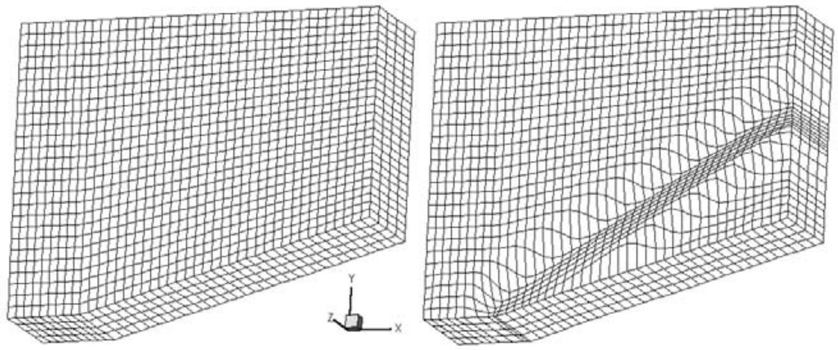

Figure 2: Initial and final mesh

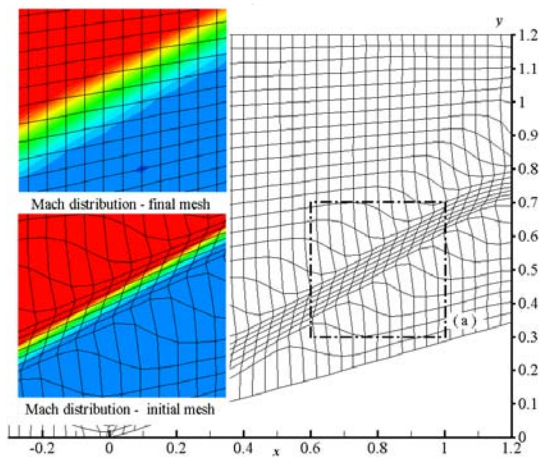

Figure 3: Final mesh and detail

4.2 Steady supersonic flow over a circular cylinder

A steady supersonic flow over a circular cylinder is analyzed in this section. The freestream flow has the following properties: Mach number $M_\infty = 3.0$ and specific mass $\rho_\infty = 1.0$. The domain is discretized using a mesh with $25 \text{ x } 5 \text{ x } 25$ elements.

In Fig. 5 the final mesh is shown, and it is observed that the elements are aligned with the shock wave conserving a mesh with a relatively good quality. The distributions of the pressure field for both, the initial and the final meshes, are shown in Fig 6, and it is observed that the proposed adaptive method improves result in regions with strong gradients.

Finally, the specific mass distribution in the stagnation line is presented in Fig. 7, where it is observed the difference between the gradients obtained with the initial and the final mesh. Results are similar to those obtained by Le Beau and Tezduyar[16].

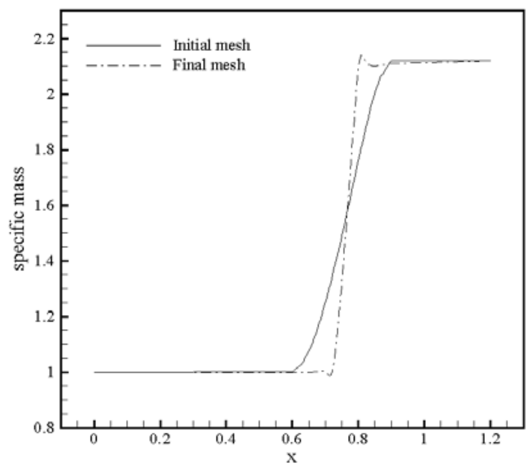

Figure 4: Distrubution of the specific mass along the $y = 0.5$

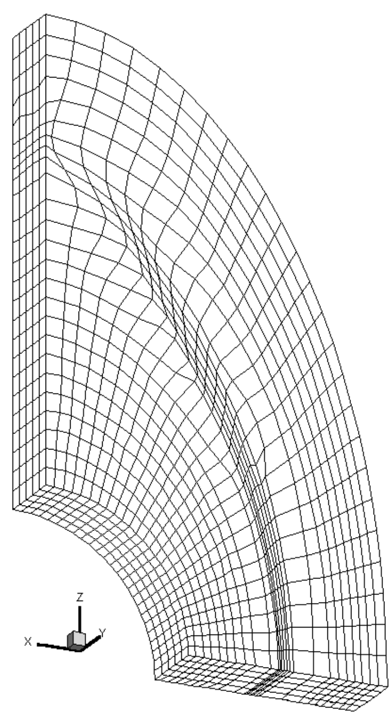

Figure 5: Final mesh after the adaptation process

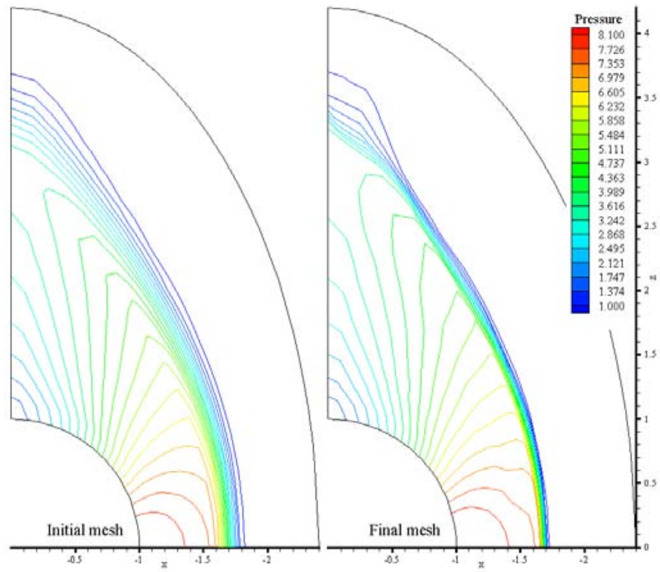

Figure 6: Comparison of the pressure distribution for both meshes

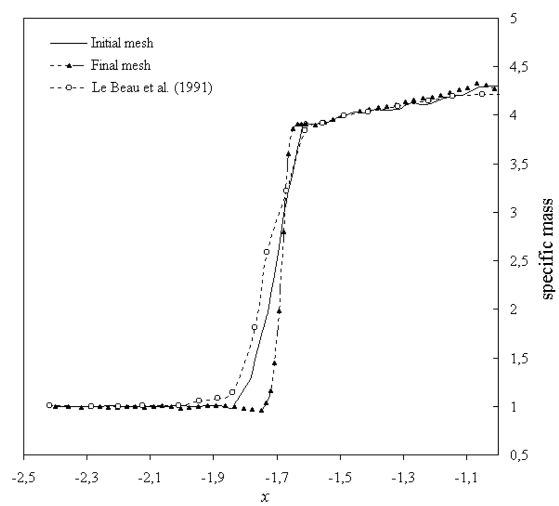

Figure 7: Specific mass distribution in the stagnation line

5 CONCLUSIONS

The development of a versatile and computationally effective methodology to adapt finite element mesh to simulate compressible flows with strong shock waves was the main objective of this work. The nodal re-allocation adaptivity, used in this study, starts from an initial mesh and the grids are concentrated in the desired region without any grid tangling. The method is characterized by error estimation measured in the element edges using a Riemann metric, which is defined employing the Hessian matrix. An optimization procedure is used to preserve as well as possible mesh orthogonality, smoothness and equidistribution of the error.

Good results for supersonic flows were found, showing that they were improved using the adaptive procedure with respect to those obtained with the initial mesh.

6 REFERENCES

[1] R. Löhner, *Applied CFD Techniques. An introduction based on Finite Element Methods*, Wiley, 2001.

[2] P.A. Gnoffo, "A finite-volume, adaptive grid algorithm applied to planetary entry flowfields", *AIAA Journal*, **21**(9), 1249-1254 (1983).

[3] K. Nakahashi and G.S. Deiwert, "Self-adaptive grid method with application to airfoil flow", *AIAA Journal*, **25**(4), 513-520 (1987).

[4] D.F. Hawken, J.J. Gottlieb and J.S. Hansen, "Review of some adaptive node-movement techniques in finite-element and finite-difference solutions of partial differential equations", *J. Comp. Physics*, **95**, 254-302 (1991).

[5] D. Ait-Ali-Yahia, W.G. Habashi and A. Tam, "A directionally adaptive methodology using an edge-based error estimate on quadrilateral grids", *Int. J. Num. Meth. Fluids*, **23**, 673-690 (1996).

[6] A Tam, D. Ait-Ali-Yahia, M.P. Robichaud, M. Moore, V. Kozel and W.G. Habashi, "Anisotropic mesh adaptation for 3D flows on structured and unstructured grids", *Comp. Meth. App. Mech. Eng.*, **189**, 1205-1230 (2000).

[7] J. Donea, "A Taylor-Galerkin method for convective transport problems", *Int. J. Num. Meth. Eng.*, **23**, 673-690 (1996).

[8] M.P. Kessler and A.M. Awruch, "Analysis of hypersonic flows using finite elements with Taylor-Galerkin scheme", *Int. J. Num. Meth. Fluids*, **44**, 1355-1376 (2004).

[9] G. Bono, *Mesh adaptation via node movement for compressible flows*, MSc Thesis, PROMEC, Federal University of Rio Grande do Sul, Brazil, 2004. (in portuguese, original title is: Adaptação via movimento de malhas em escoamentos compressíveis)

[10] J. Peraire, M. Vahdati, K. Morgan and O.C. Zienkiewicz, "Adaptive remeshing for compressible flow computations", *J. Comp. Physics*, **72**, 449-466 (1987).

[11] J.U. Brackbill and J.S. Saltzman, "Adaptive zoning for singular problems in two dimensions", *J. Comp. Physics*, **44**, 342-368 (1982).

[12] R. Carcaillet, G.S. Dulikravich and S.R. Kennon, "Generation of solution-adaptive computational grids using optimization", *Comp. Meth. App. Mech. Eng.*, **57**, 279-295 (1986).

[13] S.R. Kennon and G.S. Dulikravich, "Generation of computational grids using optimization", *AIAA Journal*, **245**, 1069-1073 (1986).

[14] W.H. Press, S.A. Teukolsky, W.T. Vetterling and B.P. Flannery, *Numerical Recipes in Fortran 77*, Cambridge University Press, 1992.

[15] NACA Report 1135, "Equations, tables, and charts for compressible flow", (1953).

[16] G.J. Le Beau and T.E. Tezduyar, “Finite-element computation of compressible flows with the SUPG formulation”, *Adv. Fin-Elem. Analysis Fluids Dynamics*, **123**, 21-27 (1991).